Photoreduction and Reoxidation of the Three Iron-Sulfur Clusters of Reaction Centers of Green Sulfur Bacteria

Pierre Sétif,* Daisuke Seo,[†] and Hidehiro Sakurai[†]

*Commissariat à l'Energie Atomique, Département de Biologie Cellulaire et Moléculaire, Section de Bioénergétique and CNRS URA 2096, 91191 Gif sur Yvette, France; [†]Department of Biology, School of Education, Waseda University, Tokyo 169-8050, Japan

ABSTRACT   Iron-sulfur clusters are the terminal electron acceptors of the photosynthetic reaction centers of green sulfur bacteria and photosystem I. We have studied electron-transfer reactions involving these clusters in the green sulfur bacterium *Chlorobium tepidum*, using flash-absorption spectroscopic measurements. We show for the first time that three different clusters, named F_X, F_1, and F_2, can be photoreduced at room temperature during a series of consecutive flashes. The rates of electron escape to exogenous acceptors depend strongly upon the number of reduced clusters. When two or three clusters are reduced, the escape is biphasic, with the fastest phase being 12–14-fold faster than the slowest phase, which is similar to that observed after single reduction. This is explained by assuming that escape involves mostly the second reducible cluster. Evidence is thus provided for a functional asymmetry between the two terminal acceptors F_1 and F_2. From multiple-flash experiments, it was possible to derive the intrinsic recombination rates between $P840^+$ and reduced iron-sulfur clusters: values of 7, 14, and 59 s^{-1} were found after one, two and three electron reduction of the clusters, respectively. The implications of our results for the relative redox potentials of the three clusters are discussed.

INTRODUCTION

Photosynthetic reaction centers $(RCs)^1$ of anaerobic green sulfur bacteria (PS-C) and photosystem I (PSI), which is found in oxygenic photosynthetic organisms, are considered to be evolutionarily related (Mathis, 1990; Nitschke and Rutherford, 1991; Blankenship, 1992; Golbeck, 1993a). They share many common features, particularly the presence of iron-sulfur clusters as low potential terminal acceptors that can reduce soluble ferredoxin (Golbeck, 1993b; Sakurai et al., 1996). The two large polypeptides that make up the RC cores show substantial sequence homology with core PSI being heterodimeric and core PS-C being presumably homodimeric (Büttner et al., 1992a). By analogy to PSI, the $(PscA)_2$ core homodimer of PS-C is thought to provide ligands for a bridging [4Fe-4S] cluster named F_X (Büttner et al., 1992b). The two terminal acceptors of PSI, named F_A and F_B, are bound to an extrinsic subunit PsaC of 9 kDa, which closely resembles bacterial 2 × [4Fe-4S] ferredoxins (Oh-oka et al., 1987). A 23-kDa subunit, named PscB, was identified in PS-C of *Chlorobium limicola* f. *thiosulfatophilum* as the counterpart of PsaC, in so far as it contains cysteine motifs for binding two [4Fe-4S] clusters (Büttner et al., 1992b).

The primary electron donors in PSI and PS-C are special pairs of chlorophyll (Chl) *a* (P700) and BChl *a* (P840), respectively. In PSI, two different types of electron acceptors, namely, a Chl *a* (named A_0) and a phylloquinone (named A_1), precede the terminal iron-sulfur cluster accep-

tors (Brettel, 1997). Although an opposite view has been put forward (Yang et al., 1998), evidence is growing that both branches related by pseudo-C_2 symmetry may be active in electron transfer in PSI (Guergova-Kuras et al., 2001), in line with a symmetrical arrangement of redox-active chlorophylls and phylloquinones (Klukas et al., 1999). The primary acceptor A_0 in PS-C is $BChl_{663}$, having the same porphyrin moiety as that of Chl *a*. The functional involvement of a quinone as a secondary acceptor in PS-C is still a matter of debate (Nitschke et al., 1987; Muhiuddin et al., 1999; Kjaer et al., 1998; Kusumoto et al., 1999).

In PS-C, the presence of two iron-sulfur clusters, equivalent to F_A and F_B of PSI and denoted (F_1, F_2) in the following, has been substantiated by several low-temperature electron paramagnetic resonance (EPR) studies (Oh-oka et al., 1993; Kusumoto et al., 1994; Scott et al., 1997, and references therein). For many years, only small signals ascribed to F_X have been observed (Oh-oka et al., 1993; Kusumoto et al., 1994; Nitschke et al., 1990; Hager-Braun et al., 1997). More recently, a F_X^- signal was reported in isolated membranes and in purified PS-C of *C. tepidum* (Vassiliev et al., 2000). There is some controversy about the EPR-monitored midpoint redox potentials E_ms of (F_1, F_2), with values below (Nitschke et al., 1990) or above (Kusumoto et al., 1994; Scott et al., 1997) −600 mV. In flash-induced absorption change measurements made at room temperature, bleaching due to reduction of a single iron-sulfur cluster has been previously reported (Kusumoto et al., 1995b). In PS-C, there are scarce and sometimes conflicting reports on recombination rates involving reduced acceptors, with halftimes ranging from 50 μs to 600 ms (reviewed in Sakurai et al., 1996). The picture is even more confused if one considers that iron-sulfur clusters may be partially destroyed in most preparations (Miller et al.,

1992; Kusumoto et al., 1995a; Francken et al., 1997; Iwaki et al., 1999; Schmidt et al., 2000).

In a previous study (Kusumoto et al., 1999), we have shown by flash-absorption spectroscopy the presence of two functionally equivalent bound cyt *c* in purified RCs of *C. tepidum*. In multiple-flash experiments that made use of the presence of the two bound cyt *c*, we also provided evidence that only three stable acceptors can be photoreduced in the micro- to millisecond time range. The chemical identity of these acceptors was not fully assessed, but the relatively slow decay rates ($t_{1/2} > 5$ ms) and the absence of absorbance changes due to menaquinone were taken as evidence that iron-sulfur clusters (ISCs) were involved. In the present study made by flash-absorption spectroscopy at room temperature, we provide direct evidence that three ISCs are functional in PS-C of *C. tepidum*. We also measure rates of electron escape to exogenous acceptors and of charge recombination reactions.

MATERIALS AND METHODS

Photochemically active PS-C complexes were prepared from *C. tepidum* under strictly anaerobic conditions as previously described (Kusumoto et al., 1994, 1999), except that all the media used from extraction with Triton X-100 and thereafter contained 10% (v/v) glycerol. The glycerol concentrations carried over into the reaction mixtures were 0.5–2% (v/v). The preparations, which were tested for cyt *c* content as detailed in Kusumoto et al. (1999), contained 2 photooxidizable cyt *c* molecules per photoactive P840. They had absorbance maxima in the near-infrared at 811–814 nm, and $A_{\approx 810}$ denotes the absorbance at the maximum. PS-C preparations were studied in a standard reaction mixture containing 50 mM Tris-HCl (pH 8.0), 0.1 mM EDTA, 2.5 mM MgCl$_2$, 0.1% Triton X-100, 5 mM D-glucose, 1.25 U of glucose oxidase, 5×10^{-3} U of catalase, 0.25% ethanol, and 0.5–2% glycerol (v/v). Experiments were made at various concentrations of sodium ascorbate and 1-methoxy-5-methylphenazinium methyl sulfate (mPMS), as indicated in figure legends.

A single set-up was used for flash-absorption measurements, except for the detecting device, which can be changed in a few minutes for measurements at different wavelengths (photomultiplier versus germanium photodiode). The measuring light was provided by a 200-W tungsten-halogen lamp, and the wavelength was selected with interference filters placed before and after the 1×1 cm square cuvette containing the sample. Filter bandwidths (full width at half-maximum) were 35 nm at 1150 nm and 5 nm or 10 nm in the blue region (5 nm at 430, 440, 450, and 460 nm; 10 nm at 400, 410, 420, and 480 nm). It was checked that, during measurements in the blue region, the measuring light had no significant actinic effect: a two-fold decrease in light intensity had no effect on the size and the decay kinetics of the observed signals. The samples were excited at 90° to the measuring beam by either ruby laser or Xe flashes. For single- or double-flash experiments, excitation was provided by one or two similar ruby laser flashes (694.3 nm; duration, 25 ns; energy, 9–13 mJ; Quantel, France) separated by an adjustable delay. For three- and four-flash experiments, a Xe flash was also used (duration, 5 μs). It was checked that both the ruby lasers and the Xe flashes saturate PS-C photochemistry. Kinetics of P840$^+$ decay were measured at 1150 nm with a germanium photodiode of 5 mm diameter (type J16–85P-R05M-HS from EG&G Judson (Montgomeryville, PA). The time resolution of the set-up was limited by the detecting diode: 4 μs for signal rise (10–90%). Assuming the published spectrum of P840$^+$ around 1150 nm (Olson et al., 1976) with $\Delta\epsilon = 21$ mM^{-1} cm^{-1} at 1157 nm and the transmission spectra of our broadband interference filters, an effective $\Delta\epsilon$ of 18.6 mM^{-1} cm^{-1} can be calculated after integration over

the bandwidths of the filters (Kusumoto et al., 1999). Kinetics of reduction of oxidized cyt *c* or reoxidation of reduced ISCs were recorded in the blue region with a photomultiplier with a response time τ of either 0.1 or 1 ms. All experiments were performed at 296 K. Decay of absorption changes were fitted with several exponential components using a Marquardt nonlinear least-squares algorithm.

RESULTS

In this study, we performed flash-absorbance measurements on a PS-C preparation from *C. tepidum* containing two bound cyt *c* per photoactive primary donor P840. Such a preparation was identical to one type of the preparations that had been described and studied previously in detail (Kusumoto et al., 1999). Such a preparation had been found to be fully photoactive with no detectable fast recombination associated with destruction of secondary acceptors. Measurements were performed either at 1150 nm, a wavelength that had been shown previously to be extremely useful to probe P840$^+$ decay (Kusumoto et al., 1999), or in the blue region for monitoring redox states of bound cyt *c* and ISCs.

Accumulation of three reduced iron-sulfur clusters during a series of flashes

To detect photoaccumulation of reduced acceptors by flash-absorption spectroscopy, we need to minimize the contribution of P840$^+$ and cyt c^+, which undergo redox equilibration with $t_{1/2} = 60$–100 μs (Kusumoto et al., 1999) and to add some exogenous donor(s) to reduce both P840$^+$ and cyt c^+. In the blue region, where reduction of ISCs leads to a bleaching, the wavelength of 440 nm is well suited as it is close to an isosbestic point of cyt *c* (Kusumoto et al., 1995b), the oxidation of which gives a very large bleaching centered at 420 nm. The experiments depicted in Fig. 1 were thus made at 440 nm in the presence of 5 μM mPMS and 5 mM ascorbate. The inset of Fig. 1 shows P840$^+$ formation and its reduction by reduced mPMS occurring with a $t_{1/2}$ of 1.4 ms. These decay kinetics were better seen after the third flash, as most of P840$^+$ was quickly reduced by cyt *c* after the first two flashes. The same sample has been studied at 440 nm on a longer time range (up to 1.5 s), allowing us to monitor exclusively the redox state of acceptors beyond 10–15 ms where contributions of oxidized P840 and cyt *c* should be negligible. After single-flash excitation (upper trace), a bleaching was observed, in accordance with reduction of an ISC, and the signal relaxed monoexponentially with a rate of 1.64 s^{-1} (continuous line). When the second flash was given 15 ms after the first one (middle trace), the total bleaching was about twice that observed after the first flash. The signal decay was very well fitted with two exponential components of similar amplitudes with rates of 19.6 and 1.61 s^{-1}. A further bleaching was observed when a third flash was given 20 ms after the second one (not shown). However, the maximal bleaching was not obtained
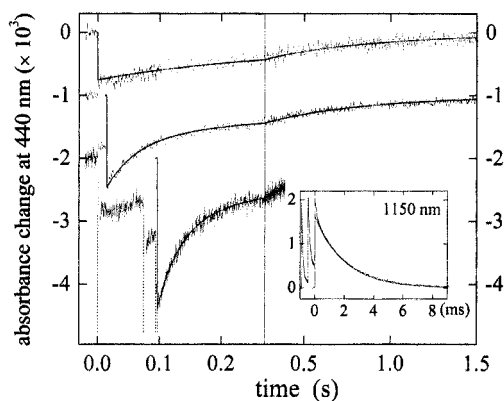
FIGURE 1 Flash-induced absorbance changes measured at 440 nm. The standard reaction mixture contained PS-C ($A_{\sim810} = 0.75$), 5 mM sodium ascorbate, and 5 μM mPMS. (*Upper trace*) Single flash experiment (ruby laser); (*middle trace*) two-flash experiment (ruby lasers, $\Delta t = 15$ ms); (*lower trace*) four-flash experiment (Xe/Xe/ruby/ruby, $\Delta t = 75$ ms/20 ms/2 ms). Averages of 6, 6, and 10 experiments for upper, middle, and lower traces, respectively. The time response of the set-up was 1 ms for the two upper traces and 100 μs for the lower one. Delay between two consecutive experiments was 15 s. The inset shows the decay of P840$^+$ at 1150 nm after three flashes ($\Delta t = 450$ μs/450 μs), average of four experiments. Fits with exponential components are superimposed on the experimental traces. (*Upper trace*) One phase (1.64 s^{-1}, -7.2×10^{-4}); (*middle trace*) two phases (19.6 s^{-1}, -8.0×10^{-4}; 1.61 s^{-1}, -6.6×10^{-4}); (*lower trace*) two phases (22.6 s^{-1}, -15.8×10^{-4}; 1.63 s^{-1}, -7.9×10^{-4}); (*inset*) one phase (489 s^{-1}, 1.62×10^{-3}). Initial amplitude of $\Delta A_{1150\ nm}$ is 2.08 $\times$ 10^{-3}, corresponding to [PS-C] = 0.112 μM. The amplitudes were obtained by extrapolating all components back to zero time.

in this experiment because part of the decay occurred with a rate of ~20 s^{-1} after the second flash. A maximal bleaching amplitude due to reduction of the third stable acceptor was obtained when a fourth flash was given to the sample 2 ms after the third one (lower trace; time intervals: 75 ms/20 ms/2 ms). This experiment makes use of the presence of the bound cytochromes, which allows us to elicit almost full charge separation during two closely separated flashes. The total bleaching observed in these four-flash experiments was about three times larger than that due to single-flash excitation. A very good fit of the decay was obtained with two exponential components with rates of 22.6 and 1.63 s^{-1}, the fast-phase amplitude being about twice as large as that of the slow phase, whereas a three-exponential fit did not give a significantly better result.

Single-flash experiments were also performed as above from 400 to 480 nm, resulting in bleaching decaying with rates of 1.4–1.9 s^{-1} as well as faster components assigned to P840$^+$ and cyt c^+ decay. The spectrum of the slow component, which is shown in Fig. 2 (circles and continuous line), is characteristic of a [4Fe-4S] cluster difference spectrum (see, e.g., Ke, 1973). Two- and four-flash experiments, similar to those shown for 440 nm in Fig. 1, were also performed at 410, 460, and 480 nm, the wavelengths at which the contributions of cyt c and P840 are relatively
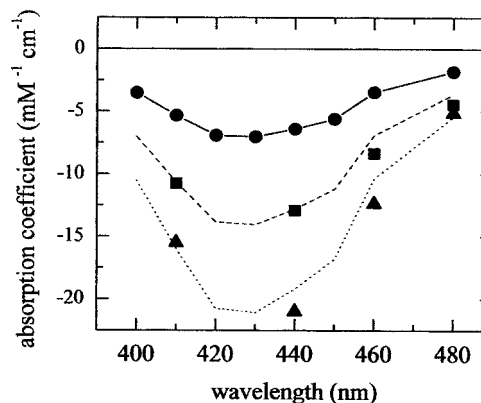
FIGURE 2 Differential absorption spectra of flash-induced bleaching between 400 and 480 nm. These spectra correspond to one (●), two (■), and four (▲) flashes in experiments similar to those described in Fig. 1. The single-flash spectrum is also shown after multiplication by factors of 2 (– – –) and 3 (· · ·). The scale is obtained from experiments made at 1150 nm for measurement of P840$^+$ decay (cf. *inset* of Fig. 1) by assuming an absorption coefficient of 18.6 mM^{-1} cm^{-1}.

small (Fowler et al., 1971; Swarthoff et al., 1981). The observed decays were similar to those found at 440 nm, and their total amplitudes are shown in Fig. 2 (squares and triangles). In the same figure, the single-flash spectrum is also shown after multiplication by factors of 2 and 3 (dashed and dotted lines, respectively).

The comparison of spectra shows that the signal profiles are very similar for the first, second, and third reduced acceptors, in accordance with their identification as [4Fe-4S] clusters. The scale of absorption coefficients used in Fig. 2 was obtained by using an effective absorption coefficient of 18.6 mM^{-1} cm^{-1} for P840$^+$ at 1150 nm, calculated by taking account the transmission spectra of the interference filters (see Materials and Methods). With this assumption, bleaching of the first reduced ISC is maximal at 430 nm with a coefficient of -7.0 mM^{-1} cm^{-1}. We stress again the observation that the bleaching increments observed after reduction of a second or third electron acceptor are similar to the bleaching observed for reduction of the first acceptor, thus providing evidence for the similar chemical nature of these three acceptors. This conclusion is independent of the absolute values of the calculated absorption coefficients.

Electron escape to exogenous acceptors

In the experiments depicted in the previous paragraph, reoxidation of reduced ISCs was relatively slow and must occur through an escape process to some exogenous acceptor as there was no more P840$^+$ or cyt c^+ available for a recombination reaction 10 ms after flash excitation. A striking feature of our observations was the change in the escape rate after reduction of the second ISC (Fig. 1) whereas reduction of the third ISC
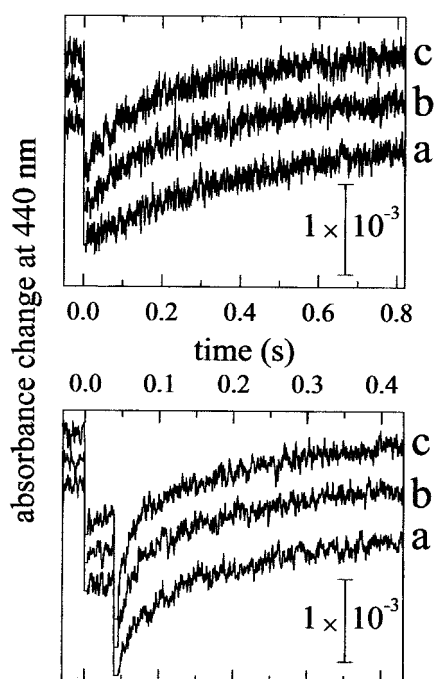
FIGURE 3 Flash-induced absorbance changes measured at 440 nm at different mPMS concentrations. The standard reaction mixture contained PS-C (0.21 μM), 5 mM sodium ascorbate, and various concentrations of mPMS: 2 μM (*traces a*), 10 μM (*traces b*), and 20 μM (*traces c*). (*Upper traces*) Single-flash experiments; (*lower traces*) double-flash experiments ($\Delta t = 40$ ms). Excitation was provided by ruby lasers. The absorption change is not shown for a period of 5 ms after flashes as the photomultiplier artifact was not subtracted (response time 1 ms).
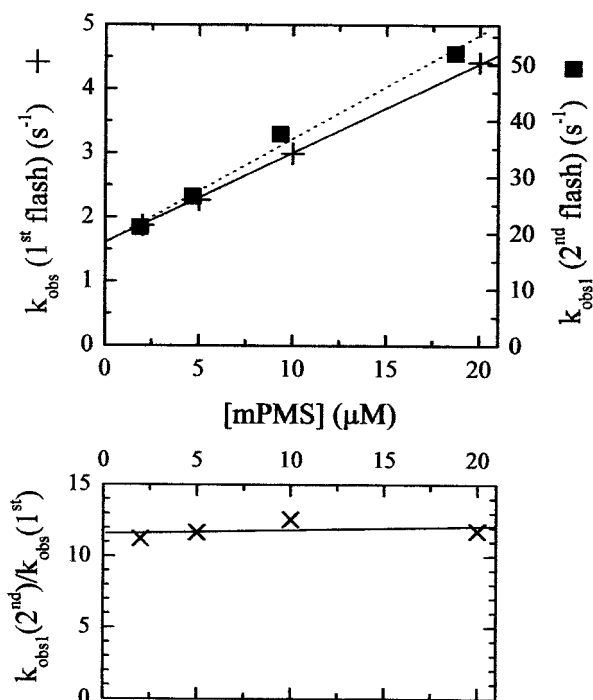

FIGURE 4 Kinetic parameters of decay of bleaching at 440 nm as a function of mPMS concentration. Kinetics as those shown in Fig. 3 were fitted either with one (first flash) or two (second flash) exponential components. (*Upper part*) +, left scale: decay rate after the first flash and slowest decay rate after the second flash (identical rates); ■, right scale: fastest decay rate after the second flash. (*Lower part*) Ratio between the fast and the slow components displayed in the upper part. Linear fits of all sets of data are also shown.

accelerated only marginally the fastest phase of escape. Such a biphasic decay receives a simple interpretation if one assumes that the fastest phase of the escape occurs as long as at least two reduced ISCs are present, whereas the escape becomes much slower as soon as there is only one reduced ISC left. To test further this effect, the escape kinetics were studied at different mPMS concentrations in single- and double-flash ($\Delta t = 40$ ms) experiments. This is shown in Fig. 3 for three different mPMS concentrations of 2, 10, and 20 μM. After the first flash, the escape was monophasic and its rate increased linearly with mPMS concentration. After the second flash, the decay was biphasic and the rates of both phases increased linearly with mPMS concentration. Moreover, the halftime of the slowest component observed after the second flash is similar to the halftime of the single decay component observed after the first flash. After the second flash, both phases were of similar amplitudes, irrespective of mPMS concentrations. The rates of the two phases observed after the second flash and the ratio between these two rates are plotted in Fig. 4 as a function of mPMS concentration. The ratio was almost [mPMS] independent with an average value of 11.7. The fact that both rates increased with mPMS indicates that some mPMS remained oxidized in the presence of 5 mM ascorbate and could accept electrons from a reduced ISC. When extrapolated to no

mPMS, escape was still occurring with rates of 1.6 and 18.2 s^{-1} for the first flash decay and the fastest phase of the second flash decay, respectively. It appears most likely that an oxidized form of ascorbate is the accepting species in the absence of mPMS as the escape rate was found to increase with increasing amounts of added ascorbate (not shown). The escape rate was also studied after reduction of all three ISCs in four-flash experiments similar to the one described in Fig. 1. At all mPMS concentrations that were tested, two decay components were observed as was the case with two reduced ISCs with the fastest component being twice as large as the slowest one. The slowest component was similar both in amplitude and halftime to the decay observed after a single flash. The fastest component had almost the same halftime ($\sim$10% increase) as the fastest component observed after the second flash, with an amplitude twice as large.

Slowly decaying components of P840$^+$ and cyt c$^+$

To study the charge recombination reactions between P840$^+$ and reduced ISCs, we performed one-, two-, and
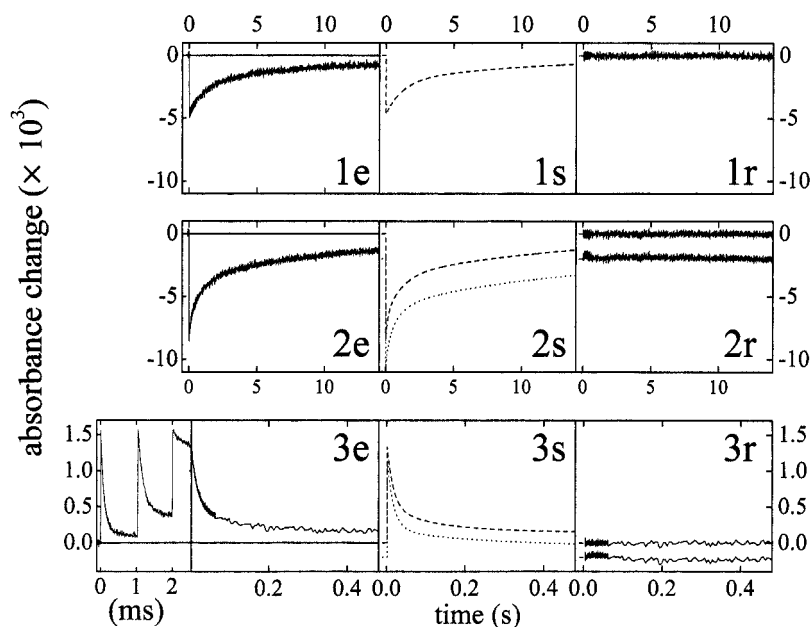
FIGURE 5 Flash-induced absorbance changes in the absence of ascorbate and mPMS. Upper, middle, and lower rows correspond to one-, two-, and three-flash experiments, respectively (one flash: ruby; two flashes: ruby with $\Delta t = 2$ ms; three flashes: ruby/Xe/ruby with $\Delta t = 1$ ms/1 ms). For one-flash and two-flash experiments, the signals that are displayed correspond to the absorbance changes measured at 420 nm minus the absorbance changes measured at 440 nm (time responses of 1 ms at both wavelengths). The signal was recorded at 1150 nm for the three-flash experiment. Experimental traces are shown in column e (*traces 1e, 2e,* and *3e*). Fitted or simulated curves and the corresponding residuals are shown in columns s and r, respectively. Fitted curves are shown as dashed lines (*upper curves* in *2s* and *3s*). *Curve 1s:* biexponential fit (0.808 s^{-1}, 56.5%; 0.076 s^{-1}, 43.5%). *Curve 2s:* Triexponential fit (6.75 s^{-1}, 22.4%; 0.875 s^{-1}, 37.4%, 0.069 s^{-1}, 40.2%). *Curve 3s:* triexponential fit (64 s^{-1}, 62.1%; 9.16 s^{-1}, 24.7%, 0.26 s^{-1}, 13.1%). For the 1150-nm measurement, only the slow decay components were considered by fitting the decay for times larger than 1 ms after the last flash and extrapolating the components to flash time. The rates obtained from the fittings were used to derive donation, escape, and recombination rates (see text), which in turn were used to simulate the complete kinetic scheme described in Fig. 6. These simulations led to simulated curves shown as dotted lines in column s (*lower curves* in *2s* and *3s*). For one flash, the simulated curve is not shown as it is identical to the fitted one. PS-C concentration, 85 nM; time interval between consecutive experiments, 40 s.

three-flash measurements on a slow time scale in the complete absence of both ascorbate and mPMS (Fig. 5, *traces 1e, 2e,* and *3e,* respectively; $\Delta t = 1/2$ ms between consecutive flashes). This allowed minimizing processes of donation by exogenous donors and of escape to exogenous acceptors (see above), both processes kinetically interfering with the recombination reactions, as detailed below. We found that the reductants carried over by the stock PS-C solution were sufficient to fully reduce P840$^+$ and cyt c^+ between consecutive experiments ($\Delta t = 40$ s). As it was previously shown (Kusumoto et al., 1999), redox equilibrium between P840 and bound cyt c is reached in less than 1 ms. After completion of the equilibrium, ~6% and 20% of P840 stays oxidized after the first and second flashes, respectively (Kusumoto et al., 1999; see Fig. 5, left part of *trace 3e*). This is followed by much slower decays of P840$^+$, from which one could get in principle the rates of recombination. However, these slow phases of P840$^+$ decay are relatively small so that it is more reliable to monitor the decay of cyt c^+ for studying the recombination processes after one or two flashes. Such experiments were performed at 420 nm

(maximum of bleaching due to oxidation of cyt c). Signals are shown in Fig. 5 (*traces 1e* and *2e*), after subtraction of the signal recorded at 440 nm to minimize the contribution from reduced ISCs (see Fig. 2). After the third flash, the cyt c^+ signal was barely larger than the second flash signal (not shown), but P840$^+$ decays mostly with slow components (>1 ms), as most of the bound cyt c was already oxidized by the preceding two flashes. Therefore, the slow decay of P840$^+$ could be reliably monitored after the third flash (*trace 3e*; 1150 nm). The first flash decay at 420 nm could be perfectly fitted with two exponential components with rates of 0.808 and 0.076 s^{-1} (amplitudes of 56.5% and 43.5%, respectively; simulated curve: 1s in Fig. 5; residuals: 1r). Three exponential components with rates of 6.75, 0.875, and 0.069 s^{-1} were necessary to fit adequately the second flash decay of cyt c^+ (amplitudes of 22.4%, 37.4%, and 40.2%, respectively; simulated curve: dashed line of 2s in Fig. 5; residuals: upper curve of 2r). Three exponential components with rates of 64, 9.16, and 0.26 s^{-1} were sufficient to fit correctly the third flash decay of P840$^+$ (amplitudes of 62.1%, 24.7%, and 13.1%, respectively;

A

$(ccP)^{3+} (F_XF_1F_2)^{3-} \xrightarrow{k_{e3}} (ccP)^{3+} (F_XF_1F_2)^{2-} \xrightarrow{k_{e2}} (ccP)^{3+} (F_XF_1F_2)^{1-} \xrightarrow{k_{e1}} (ccP)^{3+} (F_XF_1F_2)$

k_{d3} k_{r3} k_{d3} k_{r2} k_{d3} k_{r1} k_{d3}

$(ccP)^{2+} (F_XF_1F_2)^{3-} \xrightarrow{k_{e3}} (ccP)^{2+} (F_XF_1F_2)^{2-} \xrightarrow{k_{e2}} (ccP)^{2+} (F_XF_1F_2)^{1-} \xrightarrow{k_{e1}} (ccP)^{2+} (F_XF_1F_{II})$

k_{d2} $\frac{k_{r3}}{1+K_2}$ k_{d2} $\frac{k_{r2}}{1+K_2}$ k_{d2} $\frac{k_{r1}}{1+K_2}$ k_{d2}

$(ccP)^{1+} (F_XF_1F_2)^{3-} \xrightarrow{k_{e3}} (ccP)^{1+} (F_XF_1F_2)^{2-} \xrightarrow{k_{e2}} (ccP)^{1+} (F_XF_1F_2)^{1-} \xrightarrow{k_{e1}} (ccP)^{1+} (F_XF_1F_2)$

k_{d1} $\frac{k_{r3}}{1+K_1}$ k_{d1} $\frac{k_{r2}}{1+K_1}$ k_{d1} $\frac{k_{r1}}{1+K_1}$ k_{d1}

$(ccP) (F_XF_1F_2)^{3-} \xrightarrow{k_{e3}} (ccP) (F_XF_1F_2)^{2-} \xrightarrow{k_{e2}} (ccP) (F_XF_1F_2)^{1-} \xrightarrow{k_{e1}} (ccP) (F_XF_1F_2)$

B

$K_1 = 4 K_2$

$(ccP)^{3+}$ — $\binom{c^+}{c^+} P^+$

$2 k_{dC}$ k_{dP}

$k_{d3} = 2 k_{dC} + k_{dP}$

$(ccP)^{2+}$ — $\binom{c}{c}^+ P^+ \xleftrightarrow{K_2} \binom{c^+}{c^+} P$

k_{dC} k_{dP} $2 k_{dC}$

$k_{d2} = \dfrac{k_{dC} + k_{dP} + 2 k_{dC} \times K_2}{1+K_2}$

$(ccP)^{1+}$ — $\binom{c}{c} P^+ \xleftrightarrow{K_1} \binom{c}{c}^+ P$

k_{dP} k_{dC}

$k_{d1} = \dfrac{k_{dP} + k_{dC} \times K_1}{1+K_1}$
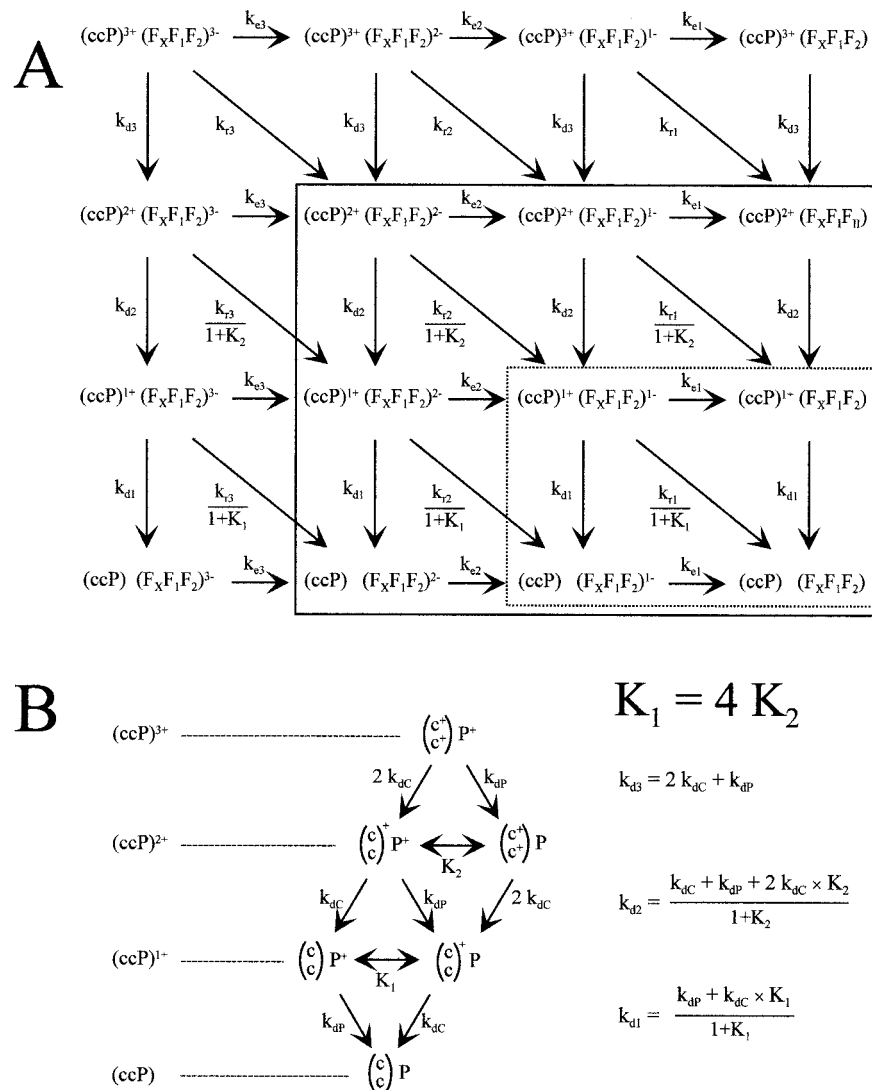
(ccP) — $\binom{c}{c} P$

FIGURE 6 Kinetic scheme of electron transfer in PS-C. (*A*) The k_{di} are rates of donation by exogenous donors, with *i* being the number of positive charges on cyt *c* (denoted c) or P840 (denoted P). The k_{ri} are rates of recombination between P840$^+$ and reduced ISCs, and k_{ei} are rates of escape to exogenous acceptors, with *i* being the number of reduced ISCs. The full scheme corresponds to triple-charge separation. Sub-schemes corresponding to single- and double-charge separations are framed with dotted and continuous lines, respectively. Fast redox equilibrium between cyt *c* and P840 is taken into account by the equilibrium constants K_1 and K_2 (cf. Appendix). (*B*) Kinetic scheme and rates of donation k_{di} for different positive charges on cyt *c* or P840, assuming fast redox equilibrium between the two species. The k_{dC} and k_{dP} are rates of donation to cyt *c*$^+$ and P840$^+$, respectively.

simulated curve: dashed line of 3s; residuals: upper curve of 3r).

Calculation of the intrinsic rates of charge recombination

We will analyze the above results of slow (cyt *c*$^+$, P840$^+$) decay to obtain the intrinsic charge recombination rates between P840$^+$ and reduced ISCs (k_{r1}, k_{r2}, and k_{r3}). Taking account of the presence of two bound cyt *c* in PS-C and of rapid redox equilibrium between P840 and cyt *c*, the full kinetic scheme that describes the present system is shown in Fig. 6 *A* with details given in the Appendix. This scheme

takes into account all reactions that must be considered for interpreting decay kinetics after one, two, or three charge separations. The complexity of this scheme has mostly two different origins.

First, it arises from the interdependence between recombination processes, donation by exogenous donors and escape to exogenous acceptors. In the present case, the last two processes cannot be neglected due to the fact that recombination reactions are relatively slow. Escape depends on the number of reduced acceptors, as depicted above (Figs. 1, 3, and 4). On the other hand, exogenous donation depends on the number of positive charges stored on cyt *c* and P840, because the proportion of the species being

TABLE 1 Kinetic characteristics of recombination rates

Number of reduced ISCs	Rate of the fastest component of decay (s^{-1})	Recombination rate (s^{-1}) (with P840$^+$ in equilibrium with cyt c)	Recombination rate (s^{-1}) (with P840$^+$)
1	0.808	$k_{r1}/(1+K_1)=0.414$	$k_{r1} = 7.0$
2	6.75	$k_{r2}/(1+K_2)=2.73$	$k_{r2} = 13.6$
3	64	$k_{r3} = 59$	$k_{r3} = 59$

reduced by the exogenous donor (either cyt c^+ or P840$^+$) will be different for different numbers of positive charges (Fig. 6 B).

Second, recombination is thought to involve only P840$^+$ and not cyt c^+. This assumption is made owing to the strong distance dependence of electron transfer (Marcus and Sutin, 1985; Moser et al., 1992; Page et al., 1999), which makes the direct recombination between a reduced ISC and cyt c^+ a very unlikely event compared with the recombination through thermal repopulation of P840$^+$ from cyt c^+. Due to fast redox equilibration between P840 and cyt c, the proportion of P840$^+$ available for recombination depends on the number of positive charges stored on cyt c and P840.

Therefore, both the exogenous donation and recombination processes are slow processes that depend upon the number of positive charges on the PS-C donors. Whereas both P840 and the two cyt c are fully oxidized after triple-charge separation, the redox equilibria after single- or double-charge separation need to be taken into account through the equilibrium constants K_1 and K_2 (Fig. 6; see Appendix). Values of 4.0 and 16.0 were taken for K_2 and K_1, respectively, in line with a ΔG^0 of -53 mV for electron transfer from one cyt c to P840$^+$ (Kusumoto et al., 1999). In the case of exogenous donation (Fig. 6 B), it is not known whether the exogenous electron donor is reducing cyt c^+ or P840$^+$ directly or both species, and we took into account both possibilities with rates k_{dC} (donation to cyt c^+) and k_{dP} (donation to P840$^+$).

The biphasic behavior observed for cyt c^+ decay after the first flash can be easily interpreted by considering the kinetic scheme framed by a dotted line in Fig. 6. Two exponential components are expected for cyt c^+ decay with rates $k_{A1} = k_{d1} + k_{e1} + k_{r1}/(1 + K_1)$ and k_{d1} (see Appendix). Moreover, the ratio between the amplitudes of the fast and the slow phases is expected to be $k_{r1}/((1 + K_1) \times k_{e1})$. This allowed us to derive all three rates: $k_{d1} = 0.076$ s^{-1}; $k_{e1} = 0.318$ s^{-1}; $k_{r1} = 7.03$ s^{-1}.

Three exponential components were necessary to fit adequately the second-flash decay of cyt c^+. The kinetic scheme after the second flash is rather complex (framed by a continuous line in Fig. 6). For P840$^+$ and cyt c^+ decay, six different exponential components are expected, including the two components that are observed after the first flash. Calculations show that these two last

components and a third one corresponding to the decay of $(ccP)^{2+}$ $(F_XF_1F_2)^{2-}$ with a rate $k_{A2} = k_{d2} + k_{e2} + k_{r2}/(1 + K_2)$ should give the major contributions. The fastest component is k_{A2}, which has a value of 6.75 s^{-1} from the fit $k_{d2} + k_{e2} + k_{r2}/(1 + K_2) = 6.75$ s^{-1}. To get k_{r2} from this equation, we need to estimate the contributions of k_{d2} and k_{e2}. In accordance with results shown above for the escape process, we took $k_{e2} = 12 \times k_{e1} = 3.82$ s^{-1}. It is shown in the Appendix that the allowable ratio k_{d2}/k_{d1} ranges between 1.9 and 3.4. With $k_{d1} = 0.076$ s^{-1}, this makes 0.145 s^{-1} < k_{d2} < 0.258 s^{-1}. This allowed us to derive the value of k_{r2}: 13.3 s^{-1} < k_{r2} < 14.0 s^{-1}. Assuming mean values of 13.6 s^{-1} and 0.2 s^{-1} for k_{r2} and k_{d2}, respectively, the cyt c^+ decay was calculated (dotted line of 2s) from the kinetic scheme of Fig. 6, by taking into account the different subpopulations of PS-C and all six exponential components (cf. Appendix). The simulated decay was very similar to the experimentally observed one, as seen from the residuals (lower curve of 2r in Fig. 5).

Three exponential components were sufficient to fit correctly the third-flash decay of P840$^+$. The full kinetic scheme of Fig. 6 corresponds to this case. This system was solved analytically, and 12 exponential components are expected for the P840$^+$ decay (see Appendix). From this analysis, it appeared that only five of these components have significant amplitudes (>4%) and that the fastest component with a rate $k_{A3} = k_{d3} + k_{e3} + k_{r3}$ should make the major contribution to the P840$^+$ decay (>60%). From the fit, the rate of this component was estimated to be 64 s^{-1}: $k_{d3} + k_{e3} + k_{r3} = 64$ s^{-1}. As shown above, the escape process is only slightly accelerated with three reduced acceptors compared with two reduced acceptors: a value of 4.3 s^{-1} was assumed for k_{e3} ($k_{e2} = 3.8$ s^{-1}). From calculations detailed in the Appendix, the ratio k_{d3}/k_{d1} should lie between 2.1 and 17. With $k_{d1} = 0.076$ s^{-1}, this made 0.16 s^{-1} < k_{d3} < 1.29 s^{-1}. This allowed us to derive the value of k_{r3} $\approx$ 59 s^{-1}. With these rates, the P840$^+$ decay was calculated (dotted line of 3s) from the kinetic scheme of Fig. 6, by taking into account the different subpopulations of PS-C and all 12 exponential components. This resulted in a simulated decay (dotted line in 3s) that was very similar to the experimentally observed one, as can be seen from the residuals (lower curve of 3r in Fig. 5). The different rates found from the above analysis are summarized in Table 1.

DISCUSSION

Three different iron-sulfur clusters are photoreducible in reaction centers of *C. tepidum*

Compared with the analogous PSI, relatively little is known concerning the low-redox-potential iron-sulfur clusters (ISCs) of reaction centers of green sulfur bacteria (PS-C). In PS-C, the presence of three different ISCs has been proposed from EPR measurements at low temperature (Oh-oka et al., 1993; Kusumoto et al., 1994; Nitschke et al., 1990). Among them, the EPR signal ascribed to the third ISC F_X has been established only recently (Vassiliev et al., 2000). These three clusters are presumably analogous to the three [4Fe-4S] clusters of PSI, named F_X, F_A, and F_B.

In the present study, we show unambiguously that it is possible to photoaccumulate three reduced ISCs at room temperature during a series of consecutive laser flashes. This evidence is based on the following observations, which were made under conditions where both $P840^+$ and cyt c^+ (in rapid redox equilibrium) are reduced rapidly by an exogenous donor (reduced mPMS): 1) the acceptor that is photoreduced after the first flash decays monoexponentially and exhibits bleaching between 400 and 480 nm, which is characteristic of that expected for reduction of a [4Fe-4S] cluster (see, e.g., Ke, 1973); 2) after two or three charge separations, the observed bleaching is two or three times larger, respectively, than the first-flash bleaching, thus indicating that a second (third) [4Fe-4S] cluster is photoreduced after the second (third) charge separation. These results show that all three ISCs are involved in forward electron transfer in PS-C at physiological temperatures. In the following, these clusters will be designated as F_X, F_1, and F_2, with the assumption that the last two species are bound to the peripheral subunit PscB. Our observations were made at room temperature, in preparations similar to those used in a previous study, where it was found that only three reduced acceptors can stably accept electrons in the microsecond-millisecond time range (Kusumoto et al., 1999). The present work ascertains that these three acceptors are ISCs, as proposed initially (Kusumoto et al., 1999). This leaves no room for menaquinone as a fourth indispensable secondary acceptor in our PS-C preparation. However, a semiquinone radical can be photoaccumulated at 205 K in membranes or reaction centers of green sulfur bacteria (Kjaer et al., 1998; Muhiuddin et al., 1999). It has been proposed that menaquinone may accept electrons from the primary acceptor A_0 in a side path of electron transfer (Hager-Braun et al., 1998).

Functional asymmetry between the terminal iron-sulfur clusters F_1 and F_2

Our observations of electron escape to exogenous acceptors can be used to derive some useful conclusions about ISCs concerning their relative accessibilities to exogenous electron acceptors and their relative redox potentials. Our data showed that escape occurs with oxidized mPMS and probably oxidized ascorbate. Escape appeared to be monophasic with one reduced ISC and biphasic with two or three reduced ISCs. When biphasic, the rate of the slowest phase was about the same as the rate of the single phase observed with one reduced ISC. A factor of ~12–14 was observed between the rates of the fastest and the slowest phases. Moreover, the ratio between the two escape rates (when biphasic) is almost constant with or without mPMS. These results indicate that the escape mechanism, and especially the ISC responsible for the escape process, is identical, irrespective of the chemical nature of the accepting exogenous species used in these experiments. Two different explanations can be proposed for the observed effects.

The above observations can be best explained by the following assumptions: 1) escape is poorly efficient after single-charge separation because the first reduced ISC (F_1 or F_2) is not accessible to exogenous acceptors, and 2) as soon as two (or three) ISCs are reduced, escape can occur from another ISC (F_2 or F_1), which is much more accessible to acceptors. Alternatively, our observations can be explained by assuming that escape always occurs from the same ISC and that a large redox shift of this ISC occurs upon reduction of the second ISC. However, this alternative is not realistic because a shift of at least −200 mV is required to explain our data (see Appendix). Such a large redox shift has not been observed during redox titrations of F_1 and F_2 of PS-C (Scott et al., 1997), making this possibility very unlikely. Thus, our data provide evidence for a functional asymmetry in accessibility of ISCs to exogenous electron acceptors. The RCs of green sulfur bacteria are thought to be able to reduce a soluble ferredoxin that is involved in $NADP^+$ reduction (Kjaer and Scheller, 1996; Seo et al., 2001). Our results suggest that reduction of soluble ferredoxin could involve a single ISC as a direct partner in electron transfer and that this ISC is the most accessible one. In the following, we will denote F_2 the most accessible ISC and F_1 the ISC that is mostly reduced upon single reduction. This behavior is reminiscent of PSI, in which F_B is the distal cluster that is the direct partner of soluble ferredoxin and is mostly responsible for electron escape to exogenous acceptors (Diaz-Quintana et al., 1998; Vassiliev et al., 1998), and F_A is the proximal cluster which is preferentially reduced at low temperature (see e.g., Golbeck, 1999). We tentatively identify F_1 to F_A and F_2 to F_B.

Intrinsic rates of charge recombination reactions between $P840^+$ and reduced clusters

Despite the inherent kinetic complexity of the kinetic system allowing us to analyze completely the slow decay phases of cyt c^+ and $P840^+$ (Fig. 6), we succeeded to derive the values of recombination rates, by choosing experimental

conditions that minimize other kinetic contributions. We found rates of 7, 14, and 59 s^{-1} for the intrinsic recombination rates k_{r1}, k_{r2}, and k_{r3} between P840$^+$ and the reduced iron-sulfur clusters after one, two, and three electron reduction of the clusters, respectively. These measurements were made possible by the quality of our PS-C preparation, which exhibits a high degree of homogeneity as far as electron transfer is concerned; this preparation contains its full complement of secondary donors and acceptors, i.e., two cyt c and three ISCs. Homogeneity most probably depends on a high degree of intactness, which was also supported by the observation that there is no detectable fast recombination between P840$^+$ and the reduced primary acceptor A$_0^-$ (Kusumoto et al., 1999). However the values of k_{r1}, k_{r2}, and k_{r3} were determined with different degrees of uncertainty. After the first flash, the decay was only biphasic and k_{r1} could be calculated relatively easily. After the third flash, the fastest component, with rate k_{A3}, was expected to make the major contribution to P840$^+$ decay in the major PS-C subpopulation, which had undergone three consecutive charge separations. Moreover, k_{r3} made the dominant contribution to k_{A3}. Therefore, we estimate that k_{r1} and k_{r3} were determined with a precision of less than 20%. The precision is not as good for k_{r2} determination as, after two charge separations, the kinetic scheme is rather complex and the fastest phase of cyt c^+ decay, which involves k_{r2}, is not the major one. Whereas the above calculations gave 13.6 s^{-1} as the most likely value of k_{r2}, kinetic simulations (not shown) performed assuming the scheme in Fig. 6 (continuous line) indicated that the limit values that are compatible with the observed kinetics are 10 $s^{-1} < k_{r2} < 25$ s^{-1}.

Rates of charge recombination: comparison with previous literature

The deduced recombination rates between P840$^+$ and reduced ISC(s) depend on the number of reduced acceptors with values of ~7, 14, and 59 s^{-1} with one, two, and three reduced ISCs, respectively. In the following, we will compare these values with previously published observations. In a purified membrane preparation from *C. vibrioforme*, Miller et al. (1992) detected some P840$^+$ decay with $t_{1/2} = 7$ ms at room temperature. Treatment of the membranes with low concentrations of a chaotrope induced appearance of a 50-μs phase. Both phases were lost at high concentrations of the chaotrope and partially restored after incubation with Fe^{3+} and SH compounds for cluster insertion. This was used to assign the 7-ms and 50-μs phases to charge recombinations within the pairs (P840$^+$ - (F$_1$, F$_2$)$^-$) and (P840$^+$ - F$_X^-$), respectively. We did not observe any 50-μs phase of significant magnitude in our PS-C, and the 7-ms phase ($k \approx 100$ s^{-1}) may well correspond to recombination between P840$^+$ and F$_X^-$ in RCs containing no bound cyt c and with destroyed (F$_1$, F$_2$). Kusumoto et al. (1995b) found that the light-induced bleaching ascribed to (F$_1$, F$_2$)$^-$ decays with $t_{1/2}$ of 400–650 ms. These measurements were made in

conditions where cyt c^+ and P840$^+$ were reduced rapidly by mPMS and ascorbate so that the decay can be ascribed mostly to reoxidation by exogenous acceptors. In PS-C from *Prosthecochloris aestuarii* containing no bound cyt, Francken et al. (1997) reported that flash-induced P840$^+$ decays at room temperature with $t_{1/2}$ of several seconds, which they explained by assuming leaking of electrons from reduced acceptors. As leaking of electrons will impede any recombination, this result cannot be usefully compared with our data. Schmidt et al. (2000) observed a component of 170 ms ($k \approx 6$ s^{-1}) during P840$^+$ reduction in the presence of dithionite and ascribed it to a recombination reaction between P840$^+$ and a reduced ISC after prereduction of another ISC. Though it is difficult to compare these observations with ours because they were made under very different experimental conditions and because their PS-C preparations are poorly characterized with respect to the number of acceptors, the 170-ms component ($k = 6$ s^{-1}) could correspond to the rate of 14 s^{-1}, which we observe with two reduced ISCs. In PS-C from *C. tepidum*, a charge recombination rate of 13 s^{-1} ($\tau = 55$ ms) at 283 K was recently reported after single-charge separation (Iwaki et al., 1999). These experiments were performed in the presence of 60% (v/v) glycerol, which inhibits electron donation by bound cyt c (Oh-oka et al., 1997). This rate is about twice as high as our estimate of 7 s^{-1} at ~295 K. This small discrepancy may be due to the fact that electron donation by exogenous donor was not taken into account in (Oh-oka et al., 1997) or to some effect of glycerol.

A number of kinetic studies have been made at temperatures of <120 K, indicating a 20–30-ms halftime for the recombination between P840$^+$ and F$_X^-$ (Miller et al., 1992; Iwaki et al., 1999; Schmidt et al., 2000; Swarthoff et al., 1981; van der Est et al., 1998). These measurements were made without prereduction of (F$_1$, F$_2$), these two ISCs being either destroyed or unable to reoxidize F$_X^-$ at low temperature. In the present study, we find a halftime of ~12 ms at room temperature for the recombination between P840$^+$ and F$_X^-$, with F$_1$ and F$_2$ being prereduced. Comparison of these data suggests that the recombination rate within the pair (P840$^+$ - F$_X^-$) is almost independent of the (F$_1$, F$_2$) redox state and of temperature. This would be consistent with a process being close to optimal ($-\Delta G \approx$ reorganization energy).

Rates of charge recombination: comparison with PSI and with heliobacterial RCs

Fast redox equilibration between P840 and cyt c decreases the probability of a wasting recombination process with effective rates $k_{r1}/(1 + K_1)$ and $k_{r2}/(1 + K_2)$ less than 0.5 and 3 s^{-1} after one and two charge separations, respectively. By comparison, recombination between P700$^+$ and (F$_A$, F$_B$)$^-$ occurs with rates between 7 and 45 s^{-1} in PSI (reviewed in Brettel, 1997). After triple-charge separation, P840$^+$ is 100% oxidized and a faster recombination rate of 59 s^{-1} is observed. This is considerably slower than what is found in PSI, where the recombination rate is ~3500 s^{-1} when both F$_A$ and F$_B$ are prereduced and ~600

s^{-1} when F_A and F_B are absent (Brettel, 1997). Such a difference may be related to the absence of a functional quinone in PS-C, contrary to PSI in which the quinone(s), named A_1, act as secondary acceptor(s) preceding the three ISCs (Brettel, 1997). It has been proposed that, at room temperature, PSI recombination reactions occur through thermal repopulation of the radical pair (P700$^+$ - A_1^-) (Brettel, 1997). This may be the dominant pathway due to the relative proximity of P700 and A_1 (Klukas et al., 1999). In the absence of such an intermediate species, recombination in PS-C would occur directly between P840$^+$ and F_X^-. In PSI, the direct recombination between P700$^+$ and F_X^- can be monitored only below 225 K. This process appears essentially temperature independent, and its rate is $\sim$10 s^{-1} (Brettel, 1997), which is only about three times slower than the low-temperature recombination in PS-C. In heliobacterial membranes and RCs, the recombination between the oxidized primary donor and F_X^- (see spectrum in Kleinherenbrink et al., 1994) occurs with a rate of 50–70 s^{-1} (Kleinherenbrink et al., 1994; Brettel et al., 1998), which is very similar to what is found in *C. tepidum*, in line with a direct recombination process not involving a quinone species (Kleinherenbrink et al., 1993).

Relative redox potentials of iron-sulfur clusters

Here we further evaluate our results to get some semi-quantitative evaluation of the relative values of the ISC redox potentials. For these evaluations, we will assume that, when considering escape and recombination processes, pre-equilibrium approximation holds for redox equilibrium between the three ISCs of PS-C. This assumption is based on the idea that both escape and recombination processes are much slower processes ($<$100 s^{-1}; these measurements) than the electron transfer between ISCs ($\gg$1000 s^{-1}), by analogy to the case of PSI (Brettel, 1997; Shinkarev et al., 2000).

Evidence was discussed above for a functional asymmetry between the terminal ISCs of PS-C with one ISC (F_2) being more accessible to exogenous acceptors and another ISC (F_1) being preferentially reduced during single reduction of the ISCs. The midpoint redox potential E_m of F_1 should be therefore higher than the redox potential of F_2. One can give an upper limit for the difference in E_m values of F_1 and F_2 by assuming that escape can occur only from F_2 and by neglecting the electrostatic interaction between F_1 and F_2 (i.e., reduction of F_1 does not modify the E_m of F_2; see discussion above). If escape occurs only from F_2, the escape observed after single reduction of the ISCs should result from thermal repopulation of the state ($F_X F_1 F_2^-$) from ($F_X F_1^- F_2$). If one neglects the contribution of the state ($F_X^- F_1 F_2$) to the redox equilibrium, the fact that escape is 12-fold slower upon single ISC reduction than upon double ISC reduction corresponds to [F_2^- F_1]/[F_2 F_1^-] = 1/12 so that $\Delta E_m = E_m(F_2) - E_m(F_1) = -\ln(12) \times RT/F = -63$ mV. If one assumes that F_X and F_2 have similar E_m values (see below), one can calculate $\Delta E_m = -\ln(12 \times 2) \times RT/F = -81$ mV.

For discussing recombination processes, one can make a realistic assumption: whatever the number of reduced ISCs is, recombination occurs only from F_X^- by thermal repopulation. This is related to the strong distance dependence of electron transfer, F_X being most probably much closer to P840 than F_1 and F_2. Within this assumption, comparison of the recombination rates after single and triple reduction of ISCs ($k_{r1} = 7$ s^{-1}; $k_{r3} = 59$ s^{-1}) allows us to calculate the amount of F_X^- thermally populated from F_1^- after single ISC reduction. This amount is 100% $\times$ 7/59 = 12% corresponding to a redox gap between F_X and the F_1 below 60 mV (-60 mV $< E_m(F_X) - E_m(F_1) < 0$). One can note that this suggests than E_m of F_X is similar to, or even higher than, that of F_2 under single ISC reduction, i.e., when F_1 is oxidized. This appears somewhat surprising both by analogy to PSI and by taking into account that no F_X^- is observed during redox titrations of ISCs in PS-C (Scott et al., 1997). However, one must note that the above estimates of relative E_m values neglect electrostatic interactions between ISCs. One can, for example, speculate that reduction of F_1 may shift the E_m of F_X to more negative values due to electrostatic interactions.

APPENDIX

In the following, it is assumed that dehydroascorbate or oxidized mPMS are reduced by a given ISC of PS-C with an observed rate k_{obs}. We will assume that electron transfer is diffusion limited; i.e., the observed rate will depend linearly on the rate k_{on} of formation of a transient complex between PS-C and the exogenous acceptor. This corresponds to the condition: $k_{on} \ll k_{off}$, k_{et}, with k_{et} and k_{off} being the intrinsic electron transfer rate and the dissociation rate k_{off} of the complex, respectively. Two different cases must be considered. 1) $k_{et} \gg k_{off}$. This will lead to $k_{obs} = k_{on}$ so that k_{et} does not influence k_{obs}. In this case, an explanation different from a redox shift of the ISC must be sought for a change in k$_{obs}$ upon reduction of F_1. 2) $k_{et} \ll k_{off}$. This will lead to $k_{obs} = k_{on} \times k_{et}/k_{off}$, and the observed rate will be proportional to k_{et}. In this case, the observed rate k_{obs} depends on the midpoint redox potential E_m of the ISC ($E_m \approx -0.6$ V), which may be modified by reduction of a neighboring ISC. 3) k_{et} and k_{off} are of comparable magnitude. This case is intermediate between 1 and 2 and an increase in k_{obs} upon reduction of a neighboring ISC by a factor f will correspond to an increase in k_{et} by a factor $>f$. Assuming that case 2 holds, we will calculate the shift of redox potential that can be expected for a 12-fold increase of k_{obs} (and k_{et}), assuming reasonable values for the free energy ΔG and the reorganization energy λ of the electron transfer reaction. We assume $\Delta G = -0.6$ eV and $\lambda = 2.0$ eV for the electron transfer rate k_{et} and $\Delta G = -0.6$ eV $+ \Delta(\Delta G)$ and the same λ for the rate $k'_{et} = k_{et} \times 12$. According to Marcus theory (Marcus and Sutin, 1985), the rate k_{et} of this process can be written: $k_{et} = A \times \exp(-(\Delta G + \lambda)^2/4\lambda k_B T)$. This formula allows us to derive $\Delta(\Delta G) = -0.20$ eV when $k'_{et}/k_{et} = 12$. A value of 2.0 eV for λ may appear high for biological electron transfer, but reduction of a small molecule such as dehydroascorbate or oxidized mPMS in a polar environment may involve a rather large λ. Taking smaller values of λ would lead to larger $|\Delta(\Delta G)|$ and would thus reinforce our conclusion about the mechanism for reduction of exogenous acceptors.

The kinetic scheme shown in Fig. 6 *A* describes the kinetic pathways in PS-C when three charge separations have been elicited by three consecutive flashes. The following assumptions were made. 1) There is a fast redox equilibration between P840 and bound cyt *c*. This is taken into account through the equilibrium constants K_1 and K_2, which describe the equilibria with one and two positives charges on P840 and cyt *c*. With a rate constant

k_1 for electron transfer from one cyt c to P840$^+$ and a rate constant of k_{-1} for the reverse process, one has $K_1 = [(cc)^+P]/[(cc)p^+] = (2 \times k_1)/k_{-1}$, $K_2 = [(c^+c^+)P]/[(cc)^+p^+] = k_1/(2 \times k_{-1})$ so that $K_1 = 4 \times K_2$ when taking into account the presence of two cyt c per P840. The interval between consecutive flashes of a series was 1 ms, which allowed full redox equilibration between P840 and cyt c, whereas no significant exogenous donation or escape could occur during this time interval. As the different rates that are explicitly considered in the scheme (k_{di}, k_{ei}, and k_{ri}) are much slower than redox equilibria between P840 and cyt c, the pre-equilibrium approximation holds for these equilibria. The values of k_1 and k_{-1} are identical to those described in a previous paper (Kusumoto et al., 1999). These values give $K_2 = 4.0$ and $K_1 = 16.0$, which correspond to a free energy change of -53 mV for electron transfer from one cyt c to P840$^+$. 2) Due to the pre-equilibrium approximation, donation rates by an external donor k_{di}, which depend on the number i of positive charges on cyt c and P840$^+$, are a linear function of the donation rates to P840$^+$ (k_{dP}) and cyt c^+ (k_{dC}) (Fig. 6 B). 3) The pre-equilibrium approximation holds also for redox equilibrium between the three ISCs of PS-C (see text). As a consequence, recombination rates k_{ri} between reduced acceptors and P840$^+$, and escape rates k_{ei} to exogenous electron acceptors, depend solely on the number i of reduced acceptors. Kinetic pathways for one and two charge separations are simpler and are framed with dotted and continuous lines, respectively. The full kinetic system shown in Fig. 6 A has been solved analytically, which was made possible by the fact that there is no reversible reaction other than those taken into account through the pre-equilibrium approximations. This is not described in detail here, and only numeric simulations of the decays are shown in Fig. 5. For P840$^+$ or cyt c^+ decay, 12 different exponential components were found that are associated with the decay of the 12 species corresponding to the three upper rows of the kinetic scheme (no P840$^+$ or cyt c^+ in the lower row). For the partial scheme associated with two charge separations (continuous frame), 6 different components were found, these components being among the 12 describing the full scheme. For the partial scheme associated with one charge separation (dotted frame, see solution below), only two components were found, these components being among the six components describing the scheme with two charge separations. After the second and third flashes, some minor subpopulations of PS-C are present. This is linked to the fast redox equilibrium between P840 and cyt c, which results in some PS-C with P840 oxidized when the second (or third) flashes are fired. A quantitative estimate of the different subpopulations has been previously given (Kusumoto et al., 1999). These different subpopulations were taken into account for simulating the cyt c^+ decay (second flash) or P840$^+$ decay (third flash), which are exhibited in Fig. 5 (lower curves in 2s and 3s).

After one charge separation (dotted frame), the two species of the upper row decay according to the following equations:

$$[(ccP)^{1+}(F_XF_1F_2)^{1-}](t) = \exp(-k_{A1} \times t),$$

assuming a value of 1 for the total population of PS-C and $k_{A1} = k_{d1} + k_{e1} + k_{r1}/(1 + K_1)$.

$$[(ccP)^{1+}(F_XF_1F_2)](t) = \{k_{e1}/(k_{A1} - k_{d1})\}$$
$$\times \{\exp(-k_{d1} \times t)$$
$$- \exp(-k_{A1} \times t)\}$$

From $[cyt\ c^+] = \{K_1/(1 + K_1)\} \times [(ccP)^{1+}]$ and $[(ccP)^{1+}] = [(ccP)^{1+}(F_XF_1F_2)^{1-}] + [(ccP)^{1+}(F_XF_1F_2)]$, one can then calculate the decay of cyt c^+:

$$[cyt\ c^+](t) = \{K_1/\{k_{e1} \times (1 + K_1) + k_{r1}\}\}$$
$$\times \{k_{e1} \times \exp(-k_{d1} \times t) + \{k_{r1}/(1 + K_1)\}$$
$$\times \exp(-k_{A1} \times t)\}$$

Donation by external donors can occur either to P840$^+$ (rate k_{dP}) or cyt c^+ (rate k_{dC}). Equations given in Fig. 6 B can be used to derive the extreme values of k_{d2} and k_{d3} that can be calculated when the value of k_{d1} is known, whereas the respective contributions of k_{dP} and k_{dC} to k_{d1} are not known.

From the two equalities:

$$k_{d2} = \{k_{dC} \times (1 + 2K_2) + k_{dP}\}/(1 + K_2)$$

and

$$k_{d1} = (k_{dC} \times K_1 + k_{dP})/(1 + K_1),$$

and with $K_1 = 16$ and $K_2 = 4$, it can be easily calculated that

$$k_{d2}/k_{d1} = 3.4 \times (1 + 9 \times \rho_{kd})/(1 + 16 \times \rho_{kd})$$

with

$$\rho_{kd} = k_{dC}/k_{dP}.$$

The k_{d2}/k_{d1} ratio decreases monotonously from 3.4 to 1.9 when ρ_{kd} increases from 0 (donation only to P840$^+$) to ∞ (donation only to cyt c^+). Similarly, $k_{d3}/k_{d1} = 17 \times (1 + 2 \times \rho_{kd})/(1 + 16 \times \rho_{kd})$. This ratio decreases monotonously from 17 to 2.125 when ρ_{kd} increases from 0 to ∞.

REFERENCES

Blankenship, R. E. 1992. Origin and early evolution of photosynthesis. *Photosynth. Res.* 33:91–111.

Brettel, K. 1997. Electron transfer and arrangement of the redox cofactors in photosystem I. *Biochim. Biophys. Acta.* 1318:322–373.

Brettel, K., W. Leibl, and U. Liebl. 1998. Electron transfer in the heliobacterial reaction center: evidence against a quinone-type electron acceptor functioning analogous to A$_1$ in photosystem I. *Biochim. Biophys. Acta.* 1363:175–181.

Büttner, M., D. L. Xie, H. Nelson, W. Pinther, G. Hauska, and N. Nelson. 1992a. The photosystem I-like P840-reaction center of green sulfur bacteria is a homodimer. *Biochim. Biophys. Acta.* 1101:154–156.

Büttner, M., D. L. Xie, H. Nelson, W. Pinther, G. Hauska, and N. Nelson. 1992b. Photosynthetic reaction center genes in green sulfur bacteria and in photosystem 1 are related. *Proc. Natl. Acad. Sci. U.S.A.* 89: 8135–8139.

Diaz-Quintana, A., W. Leibl, H. Bottin, and P. Sétif. 1998. Electron transfer in photosystem I reaction centers follows a linear pathway in which iron-sulfur cluster F$_B$ is the immediate electron donor to soluble ferredoxin. *Biochemistry.* 37:3429–3439.

Fowler, C. F., N. A. Nugent, and R. C. Fuller. 1971. The isolation and characterization of a photochemically active complex from *Chloropseudomonas ethylica. Proc. Natl. Acad. Sci. U.S.A.* 68:2278–2282.

Francken, C., H. P. Permentier, E. M. Franken, S. Neerken, and J. Amesz. 1997. Isolation and properties of photochemically active reaction center complexes from the green sulfur bacterium *Prosthecochloris aestuarii. Biochemistry.* 36:14167–14172.

Golbeck, J. H. 1993a. Shared thematic elements in photochemical reaction centers. *Proc. Natl. Acad. Sci. U.S.A.* 90:1642–1646.

Golbeck, J. H. 1993b. The structure of photosystem I. *Curr. Opin. Struct. Biol.* 3:508–514.

Golbeck, J. H. 1999. A comparative analysis of the spin state distribution of in vitro and in vivo mutants of PsaC: a biochemical argument for the sequence of electron transfer in photosystem I as F$_X$ → F$_A$ → F$_B$ → ferredoxin/flavodoxin. *Photosynth. Res.* 61:107–114.

Guergova-Kuras, M., B. Boudreaux, A. Joliot, P. Joliot, and K. Redding. 2001. Evidence for two active branches for electron transfer in photosystem I. *Proc. Natl. Acad. Sci. U.S.A.* 98:4437–4442.

Hager-Braun, C., N.-U. Frigaard, H. P. Permentier, K. A. Schmidt, G. Hauska, J. Amesz, and M. Miller. 1998. Occurrence and function of quinones in the reaction center of *Chlorobium tepidum*. *In* Photosynthesis: Mechanisms and Effects. G. Garab, editor. Kluwer Academic Publishers, Dordrecth, The Netherlands. 555–558.

Hager-Braun, C., U. Jarosch, G. Hauska, W. Nitschke, and A. Riedel. 1997. EPR studies of the terminal electron acceptors of the green sulfur bacterial reaction center: revisited. *Photosynth. Res.* 51:127–136.

Iwaki, M., S. Itoh, S. Kamei, H. Matsubara, and H. Oh-oka. 1999. Time-resolved spectroscopy of chlorophyll-a like electron acceptor in the reaction center complex of the green sulfur bacterium *Chlorobium tepidum*. *Plant Cell Physiol.* 40:1021–1028.

Ke, B. 1973. Primary electron acceptor of photosystem I. *Biochim. Biophys. Acta.* 301:1–33.

Kjaer, B., N.-U. Frigaard, F. Yang, B. Zybailov, M. Miller, J. H. Golbeck, and H. V. Scheller. 1998. Menaquinone-7 in the reaction center complex of the green sulfur bacterium *Chlorobium vibrioforme* functions as the electron acceptor A_1. *Biochemistry.* 37:3237–3242.

Kjaer, B. and H. V. Scheller. 1996. An isolated reaction center complex from the green sulfur bacterium *Chlorobium vibrioforme* can photoreduce ferredoxin at high rates. *Photosynth. Res.* 47:33–39.

Kleinherenbrink, F. A. M., H.-C. Chiou, R. LoBrutto, and R. E. Blankenship. 1994. Spectroscopic evidence for the presence of an iron-sulfur center similar to F_X of photosystem I in *Heliobacillus mobilis*. *Photosynth. Res.* 41:115–123.

Kleinherenbrink, F. A. M., I. Ikegami, A. Hiraishi, S. C. M. Otte, and J. Amesz. 1993. Electron transfer in menaquinone-depleted membranes of *Heliobacterium chlorum*. *Biochim. Biophys. Acta.* 1142:69–73.

Klukas, O., W. D. Schubert, P. Jordan, N. Krauss, P. Fromme, H. T. Witt, and W. Saenger. 1999. Localization of two phylloquinones, Q_K and Q_K', in an improved electron density map of photosystem I at 4-Å resolution. *J. Biol. Chem.* 274:7361–7367.

Kusumoto, N., K. Inoue, H. Nasu, and H. Sakurai. 1994. Preparation of a photoactive reaction center complex containing photoreducible Fe-S centers and photooxidizable cytochrome c from the green sulfur bacterium *Chlorobium tepidum*. *Plant Cell Physiol.* 35:17–25.

Kusumoto, N., K. Inoue, H. Nasu, A. Tomioka, and H. Sakurai. 1995a. Biochemical and optical studies of photoactive reaction center complex from the green sulfur bacterium *Chlorobium tepidum*. *In* Photosynthesis: From Light to Biosphere. P. Mathis, editor. Kluwer, Dordrecht, The Netherlands, 203–206.

Kusumoto, N., K. Inoue, and H. Sakurai. 1995b. Spectroscopic studies of bound cytochrome c and an iron-sulfur center in a purified reaction center complex from the green sulfur bacterium *Chlorobium tepidum*. *Photosynth. Res.* 43:107–112.

Kusumoto, N., P. Sétif, K. Brettel, D. Seo, and H. Sakurai. 1999. Electron transfer kinetics in purified reaction centers from the green sulfur bacterium *Chlorobium tepidum* studied by multiple-flash excitation. *Biochemistry.* 38:12124–12137.

Marcus, R. A. and N. Sutin. 1985. Electron transfers in chemistry and biology. *Biochim. Biophys. Acta.* 811:265–322.

Mathis, P. 1990. Compared structure of plant and bacterial photosynthetic reaction centers. Evolutionary implications. *Biochim. Biophys. Acta.* 1018:163–167.

Miller, M., X. Liu, S. W. Snyder, M. C. Thurnauer, and J. Biggins. 1992. Photosynthetic electron-transfer reactions in the green sulfur bacterium *Chlorobium vibrioforme*: evidence for the functional involvement of iron-sulfur redox centers on the acceptor side of the reaction center. *Biochemistry.* 31:4354–4363.

Moser, C. C., J. M. Keske, K. Warncke, R. S. Farid, and L. Dutton. 1992. Nature of biological electron transfer. *Nature.* 355:796–802.

Muhiuddin, I. P., S. E. J. Rigby, M. C. W. Evans, J. Amesz, and P. Heathcote. 1999. ENDOR and special TRIPLE resonance spectroscopy of photoaccumulated semiquinone electron acceptors in the reaction centers of green sulfur bacteria and heliobacteria. *Biochemistry.* 38: 7159–7167.

Nitschke, W., U. Feiler, W. Lockau, and G. Hauska. 1987. The photosystem of the green sulfur bacterium *Chlorobium limicola* contains two early electron acceptors similar to photosystem I. *FEBS Lett.* 218: 283–286.

Nitschke, W., U. Feiler, and A. W. Rutherford. 1990. Photosynthetic reaction center of green sulfur bacteria studied by EPR. *Biochemistry.* 29:3834–3842.

Nitschke, W. and A. W. Rutherford. 1991. Photosynthetic reaction centers: variations on a common structural theme? *Trends Biochem. Sci.* 16: 241–245.

Oh-oka, H., M. Iwaki, and S. Itoh. 1997. Viscosity dependence of the electron transfer rate from bound cytochrome c to P840 in the photosynthetic reaction center of the green sulfur bacterium *Chlorobium tepidum*. *Biochemistry.* 36:9267–9272.

Oh-oka, H., S. Kakutani, H. Matsubara, R. Malkin, and S. Itoh. 1993. Isolation of the photoactive reaction center complex that contains three types of Fe-S centers and a cytochrome c subunit from the green sulfur bacterium *Chlorobium limicola* f. *thiosulfatophilum*, strain Larsen. *Plant Cell Physiol.* 34:93–101.

Oh-oka, H., Y. Takahashi, K. Wada, H. Matsubara, K. Ohyama, and H. Ozeki. 1987. The 8 kDa polypeptide in photosystem I is a probable candidate of an iron-sulfur center protein coded by the chloroplast gene frxA. *FEBS Lett.* 218:52–54.

Olson, J. M., R. C. Prince, and D. C. Brune. 1976. Reaction-center complexes from green bacteria. *Brookhaven Symp. Biol.* 28:238–245.

Page, C. C., C. C. Moser, X. X. Chen, and P. L. Dutton. 1999. Natural engineering principles of electron tunnelling in biological oxidation-reduction. *Nature.* 402:47–52.

Sakurai, H., N. Kusumoto, and K. Inoue. 1996. Function of the reaction center of green sulfur bacteria. *Photochem. Photobiol.* 64:5–13.

Schmidt, K. A., S. Neerken, H. P. Permentier, C. Hager-Braun, and J. Amesz. 2000. Electron transfer in reaction center core complexes from the green sulfur bacteria *Prosthecochloris aestuarii* and *Chlorobium tepidum*. *Biochemistry.* 39:3297–3303.

Scott, M. P., B. Kjaer, H. V. Scheller, and J. H. Golbeck. 1997. Redox titration of two [4Fe-4S] clusters in the photosynthetic reaction center from the anaerobic green sulfur bacterium *Chlorobium vibrioforme*. *Eur. J. Biochem.* 244:454–461.

Seo, D., A. Tomioka, N. Kusumoto, M. Kamo, I. Enami, and H. Sakurai. 2001. Purification of ferredoxins and their reaction with purified reaction center complex from the green sulfur bacterium *Chlorobium tepidum*. *Biochim. Biophys. Acta.* 1503:377–384.

Shinkarev, V. P., I. R. Vassiliev, and J. H. Golbeck. 2000. A kinetic assessment of the sequence of electron transfer from F_X to F_A and further to F_B in photosystem I: the value of the equilibrium constant between F_X and F_A. *Biophys. J.* 78:363–372.

Swarthoff, T., K. M. Van der Veek-Horsley, and J. Amesz. 1981. The primary charge separation, cytochrome oxidation and triplet formation in preparations from the green photosynthetic bacterium *Prosthecochloris aestuarii*. *Biochim. Biophys. Acta.* 635:1–12.

van der Est, A., C. Hager-Braun, W. Leibl, G. Hauska, and D. Stehlik. 1998. Transient electron paramagnetic resonance spectroscopy on green-sulfur bacteria and heliobacteria at two microwave frequencies. *Biochim. Biophys. Acta.* 1409:87–98.

Vassiliev, I. R., Y. S. Jung, F. Yang, and J. H. Golbeck. 1998. PsaC subunit of photosystem I is oriented with iron-sulfur cluster F_B as the immediate electron donor to ferredoxin and flavodoxin. *Biophys. J.* 74:2029–2035.

Vassiliev, I. R., M. T. Ronan, G. Hauska, and J. H. Golbeck. 2000. The bound electron acceptors in green sulfur bacteria: resolution of the g-tensor for the F_X iron-sulfur cluster in *Chlorobium tepidum*. *Biophys. J.* 78:3160–3169.

Yang, F., G. Z. Shen, W. M. Schluchter, B. L. Zybailov, A. O. Ganago, I. R. Vassiliev, D. A. Bryant, and J. H. Golbeck. 1998. Deletion of the PsaF polypeptide modifies the environment of the redox-active phylloquinone A_1. Evidence for unidirectionality of electron transfer in photosystem I. *J. Phys. Chem. B.* 102:8288–8299.